Elastic Stability of Thin-Walled Cylindrical and Conical Shells under Combined External Pressure and Axial Compression

V. I. WEINGARTEN*
University of Southern California, Los Angeles, Calif.

AND

PAUL SEIDE†
Aerospace Corporation, El Segundo, Calif.

The results of an extensive experimental program on the stability of cylindrical and conical shells under external pressure and combined external pressure and axial compression are presented. The use of the given data is discussed, and recommendations are given.

Nomenclature

D = flexural stiffness of shell wall $Et^3/[12(1 - \nu^2)]$
E = Young's modulus of shell wall material
L = axial length of cylinder or cone
l = slant length of cone
n = number of circumferential waves in cone buckled under external pressure
$\bar{n}$ = number of circumferential waves in equivalent cylinder buckled under external pressure
P_0 = critical axial compression load
p = total axial load at buckling
P = uniform internal or external hydrostatic pressure
p_{cr}, p_0 = critical external pressure
p_e = critical external pressure for equivalent cylinder
R = cylinder radius
R_1 = radius of small end of cone
R_2 = radius of large end of cone
t = shell wall thickness
α = semivertex angle of cone
ν = Poisson's ratio of wall material
ρ_{av} = average radius of curvature of cone $(R_1 + R_2)/2 \cos\alpha$

Introduction

THE problem of the buckling of conical shells under external uniform hydrostatic pressure has been studied theoretically by many investigators. The various investigations are summarized in Ref. 1, which also presents the results of a more accurate independent analysis. The conclusion reached in Ref. 1 is that the critical external pressure of a conical frustum is approximately equal to a factor times the critical external pressure of a cylinder having the same wall thickness, a radius equal to the average radius of curvature of the cone, and a length equal to the slant length of the frustum. The factor is a function only of the ratio of the end radii of the cone and increases from 1.00 for the cylinder ($1 - R_1/R_2 = 0$) to 1.22 for a cone with $1 - R_1/R_2$ equal to 0.8 and then decreases to about 1.17 for a complete cone ($1 - R_1/R_2 = 1.0$). Lower values of the factor are implied by the studies of Niordson[2] and Bijlaard,[3] but these cannot be regarded as theoretically accurate since Niordson makes many approximations of unknown effect in his analysis, whereas Bijlaard's values are based on intuition. The present investigation was designed to explore the conclusions of Ref. 1.

Presented as Preprint 65-78 at the AIAA 2nd Aerospace Sciences Meeting, New York, N. Y., January 25–27, 1965; revision received January 11, 1965. The work contained in this paper was performed at TRW Space Technology Laboratories, Inc. under Contract No. AF 04(657)-619.

* Assistant Professor, Department of Civil Engineering. Member AIAA.

† Staff Engineer, Solid Mechanics Department. Associate Fellow Member AIAA.

The theoretical small-deflection behavior of cylinders under axial compression and external uniform hydrostatic pressure is discussed in Refs. 4 and 5 and is more thoroughly investigated for both cylinders and cones in Ref. 6. The results indicate that the interaction curve is nearly a straight line for cylinders and becomes more concave downward as the taper ratio $(1 - R_1/R_2)$ increases for conical shells. No experimental data have appeared in the literature to deny or confirm these results.

Experimental Technique

The specimens used in the experiments were made of Mylar polyester sheet. This has been found to have a Young's modulus of approximately 700,000 psi, a Poisson's ratio of 0.3, and proportional limit and yield stresses of 6000 and 11,000 psi, respectively. Because of the small variation of the properties of Mylar from roll to roll, the modulus of elasticity was determined by using a load-deflection curve for each specimen.

Specimens were made by cutting accurately developed cones and cylinders from the Mylar sheet, allowing $\frac{1}{2}$ in. on the top and a minimum of $\frac{3}{4}$ in. on the bottom for clamping and a $\frac{3}{4}$-in. overlap for the longitudinal seam. All the cones were made with the same base radius to reduce the number of base clamping fixtures needed. The developed cone was then wrapped firmly about a conical wooden mandrel. A lap joint fastened with double-backed adhesive cellophane tape was used for the longitudinal seam. In later tests, the bonding material was changed to Eccobond, an epoxy cement, after experimentation with various bonding agents. Although the thin Mylar sheet is quite flexible, the use of carefully laid out patterns and conical assembly mandrels made it possible to obtain specimens that were dimensionally accurate and relatively free of initial wrinkles or bulges.

The Mylar specimens were first fixed in the upper clamping fixture and then placed on the inner portion of the lower clamping fixture, which was raised approximately two inches above the base of the loading fixture by two parallel rectangular blocks. This prevented the bottom of the cone from pressing on the base of the loading fixture. The outer portion of the clamp was then placed over the cone and brought down loosely on the top of the inner lower clamp (see Fig. 1), since it was discovered that, if the lower clamps were fastened by screws, dimples appeared and produced premature buckling as the cones were loaded. The equivalent of external pressure was supplied by evacuating the interior of the specimen by means of a vacuum pump until buckles appeared.

A number of thin-gage and thick-gage cones of various semivertex angles were tested with the outer portion of the bottom clamp removed. It was discovered that, as long as the cone was dimple-free, the buckling pressure was the same for 10°. 20°, and 30° whether or not the outer bottom clamp

was placed over the cone. For 45° and 60° cones, appreciably higher buckling pressures were obtained with the outer portion of the bottom clamp placed over the cones.

In later tests the clamping fixtures were replaced by machined metal end plates containing a circular trough. The ends of each specimen were placed in these troughs, which were then filled with a low melting point alloy. A detailed discussion of the specimen fabrication and clamping techniques is given in Ref. 7.

Results for Hydrostatic Pressure

The data for the various tests carried out in the present investigation are tabulated in Ref. 7 in the form of corresponding values of p_{cr}/p_e and $1 - R_1/R_2$. Values of p_e for the average cylinder were obtained from the analysis of Batdorf.[8] In the notation of the present paper,

$$p_e = \frac{E}{[12(1-\nu^2)]^{1/2}} \left(\frac{t}{\rho_{av}}\right)^2 \frac{1}{\frac{1}{2} + (\bar{n}l/\pi\rho_{av})^2} \times \left\{ \frac{[1 + (\bar{n}/\pi\rho_{av})^2]^2}{\{[12(1-\nu)]^{1/2}/\pi^2\}\ (l/\rho_{av})^2\ (\rho_{av}/t)} + \frac{\{[12(1-\nu^2)]^{1/2}/\pi^2\}\ (l/\rho_{av})^2\ (\rho_{av}/t)}{[1 + (\bar{n}l/\pi\rho_{av})^2]^2} \right\} \quad (1)$$

The number of circumferential waves $\bar{n}$ was varied until a minimum value of p_e was obtained.

Let us first consider the cylindrical specimens. The experimental results are compared with the theoretical curve of Ref. 8 in Fig. 2. Also shown in Fig. 2 are the experimental results of Windenberg and Trilling[9] and of Sturm.[10] It can be seen that the scatter of the present Mylar and steel results is of the same order as that obtained previously for aluminum and steel specimens. Part of the scatter for the results may be attributed to uncertainty in the modulus of elasticity, for which an average value was used for each thickness. However, there are at least two additional sources of scatter which should be noted. One factor, the effect of initial imperfections, has only recently been explored in some detail. Whereas initial imperfections of the shape of the buckle pattern have been found to have only a small effect on the critical pressure, Kempner[19] has noted that asymmetric imperfections may result in significant increases or decreases in buckling pressure. The data available is insufficient, but a grouping of the Mylar data indicates a possible dependence on radius-thickness ratio. A second source of error is the difficulty in some cases of defining a buckling pressure. For the thicker cylinders and cones, buckling was well defined, with many buckles appearing suddenly at some critical pressure. With the thinner cones however, buckling occurred in a

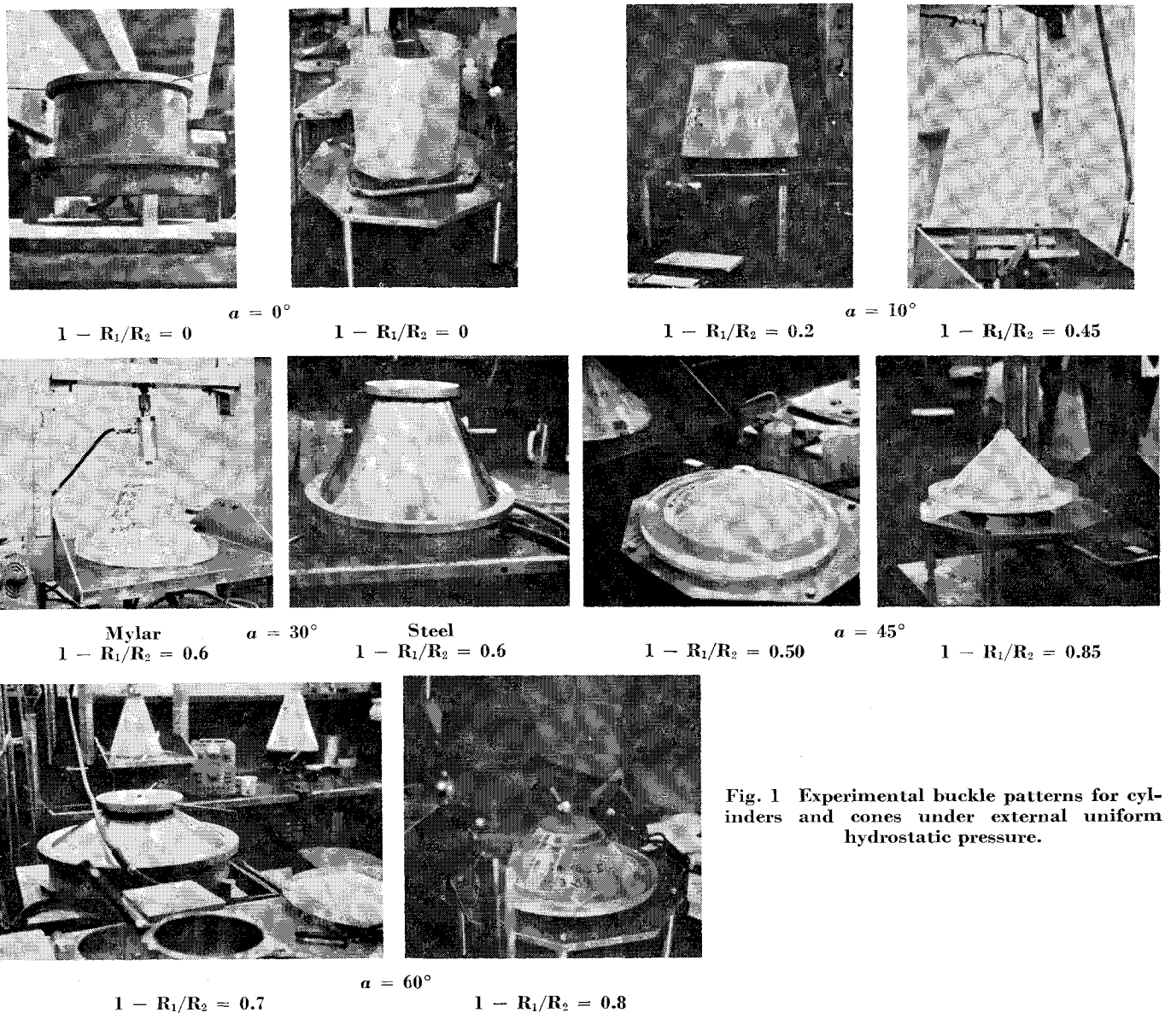

Fig. 1 Experimental buckle patterns for cylinders and cones under external uniform hydrostatic pressure.

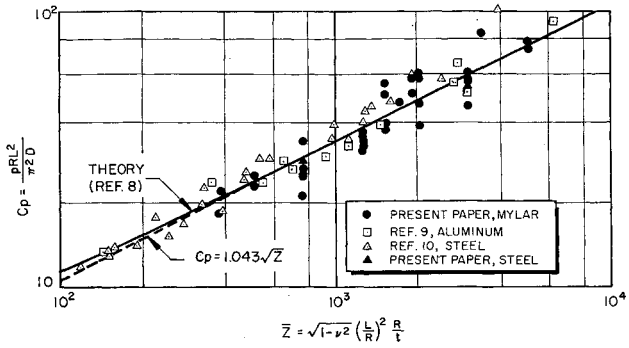

Fig. 2 Comparison with theory of various external hydrostatic pressure test results for cylinders.

progressive fashion, with an isolated buckle appearing at a low pressure, a few more at a somewhat higher pressure, and more at still higher pressures. The definition of buckling pressure for these cases was, as can be seen, a matter of individual judgment which may have varied from specimen to specimen.

The results for conical shells are shown in Fig. 3, together with values obtained by other investigators,[11–18] with theoretical results of Refs. 1–3. We see from Fig. 3 that the scatter of the data is too large to verify the trends indicated by the theory of Ref. 1. The results do indicate that Niordson's approximation yields a fairly good average fit to the data since the scatter about the line $p_{cr}/p_e = 1$ is relatively uniform for both cones and cylinders of many materials over most of the range of $1 - R_1/R_2$. Since most of the results fall within 80% of the line $p_{cr}/p_e = 1$, it is recommended that both conical shells and cylinders be designated by the formula

$$p_{cr} = 0.8\, p_e \tag{2}$$

where p_e can be obtained from Eq. (1) or from the approximate relation

$$p_e = \frac{0.92\, E}{(l/\rho_{av})(\rho_{av}/t)^{5/2}} \tag{3}$$

The buckled shapes of various cylinders and cones are shown in Fig. 1. It can be seen that the point of maximum deflection has a tendency to shift toward the large radius of the cone as the small radius decreases, as predicted in Ref. 1. The number of circumferential buckling waves were obtained experimentally and tabulated in Ref. 7.‡ The experimental

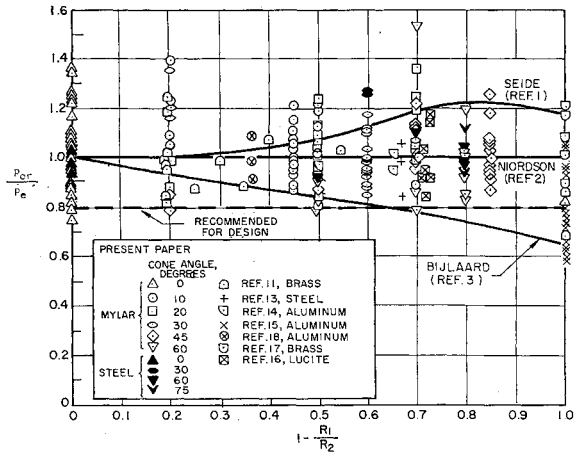

Fig. 3 Comparison with various theoretical results of external pressure test data for conical shells.

‡ Typical tabulations of the data appear in Table 1 for Mylar specimens and Table 2 for steel specimens.

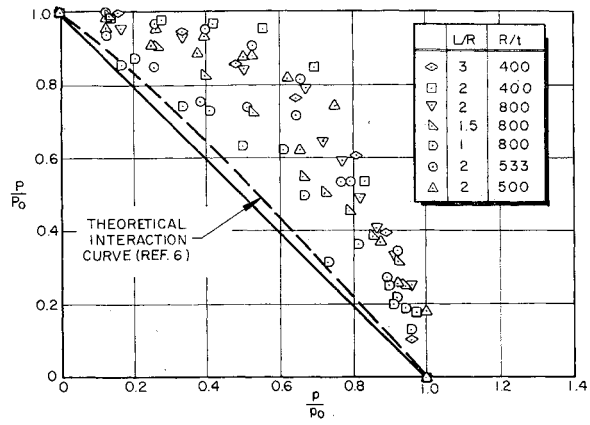

Fig. 4 Interaction curves for cylinders under axial compression and uniform external hydrostatic pressure.

data were in fair agreement with analytical predictions for the number of circumferential waves obtained from Eq. 1. The experimental results were found to be somewhat lower in most cases. The theory of Ref. 1 predicts an increase in the wave number n from that given by $\bar{n}\cos\alpha$ for values of $1 - R_1/R_2$ greater than 0.6. Experimental results, tabulated in Ref. 7, did not indicate any such phenomenon.

Results for Combined Axial Compression and External Pressure

The experimental program discussed herein is very limited, comprising 10 cylinders, 6 cones having a 30° semivertex angle, and 3 cones having a 60° semivertex angle. The results for cylinders are plotted in several different ways. For the purpose of constructing interaction curves, corresponding values of P/P_0 and p/p_0 are shown in Fig. 4. It is apparent that the spread of the data is so great that no single interaction curve can be drawn. The reason for this spread of data is more readily seen from the values of $P/2\pi Et^2$ plotted as a function of p/p_0§ in Fig. 5. Also shown is the theoretical interaction curve obtained in Ref. 6. It can be seen that, for values of external pressure near the critical value, the data follow the theoretical interaction curve reasonably well. Those cylinders that yield a lower axial buckling coefficient depart from the theoretical interaction curve much sooner than do those that

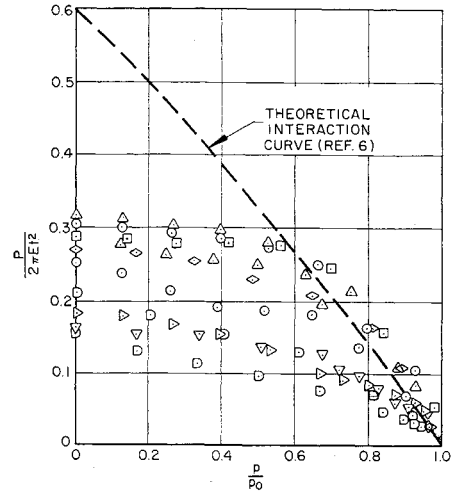

Fig. 5 Variation of axial compression coefficient with external pressure ratios.

§ p/p_e could also have been used, but with somewhat more scatter.

Table 1 Experimental data for Mylar cylinders and cones under external uniform hydrostatic pressure

t, in.	$E \times 10^{-3}$, psi	R/t[a]	L/R[a]	p_{cr}/p_e	n (experimental)	n (computed)	$\bar{Z}$	C_p
			a) $\alpha = 0°$					
0.010	690	400	1	0.895	10	12	382	18.2
0.010	690	400	1	1.087	9	12	382	22.1
0.0075	770	533	1	0.983	11	13	508	23.1
0.0075	770	533	1	1.079	11	13	508	25.4
0.005	750	800	1	0.882	11	14	763	25.4
0.005	750	800	1	0.941	12	14	763	27.1
0.005	750	800	1	0.740	...	14	763	21.3
0.005	750	800	1	1.161	...	14	763	33.5
0.003	775	1333	1	0.967	13	16	1272	36.0
0.003	775	1333	1	0.901	13	16	1272	33.5
0.003	775	1333	1	0.901	13	16	1272	33.5
0.003	775	1333	1	0.882	13	16	1272	32.8
0.003	775	1333	1	0.844	13	16	1272	31.4
0.003	775	1333	1	0.948	13	16	1272	35.3
0.005	750	800	1.5	1.078	...	...	1717	46.6
0.010	690	400	2	0.991	6	9	1526	39.5
0.010	690	400	2	0.969	6	9	1526	37.3
0.010	675	400	2	1.227	8	9	1526	50.0
0.010	675	400	2	1.340	8	9	1526	54.6
0.0080	762	500	2	1.094	8	9	1908	49.8
0.0080	712	500	2	1.232	9	9	1908	56.1
0.0075	800	533	2	1.220	9	9	2034	57.4
0.0075	800	533	2	1.253	8	9	2034	58.9
0.0075	770	533	2	0.983	7	9	2034	46.2
0.0075	770	533	2	0.811	7	9	2034	38.1
0.0050	750	800	2	1.029	8	10	3053	59.3
0.0050	750	800	2	0.951	8	10	3053	54.8
0.0050	750	800	2	0.787	...	10	3053	45.3
0.0030	775	1333	2	1.043	9	12	5086	77.6
0.0030	775	1333	2	0.977	9	12	5086	72.7
0.0100	690	400	3	1.354	...	...	3434	82.7

t, in.	$E \times 10^{-3}$, psi	ρ_{av}/t	l/ρ_{av}	$1 - R_1/R_2$[b]	p_{cr}/p_e	n (experimental)	n (predicted)
			b) $\alpha = 30°$				
0.003	775	1735	0.50	0.20	1.166	21	20–21
0.003	775	1735	0.50	0.20	1.195	21	20–21
0.005	750	1041	0.50	0.20	0.980	...	...
0.010	690	521	0.50	0.20	1.349	...	...
0.003	775	1430	1.15	0.50	0.929	11	13–14
0.003	775	1430	1.15	0.50	0.948	11	13–14
0.005	750	858	1.15	0.50	0.917	...	...
0.010	690	429	1.15	0.50	1.008	...	...
0.002	740	2020	1.48	0.60	0.844	11	13
0.002	740	2020	1.48	0.60	0.913	11	13
0.003	775	1350	1.48	0.60	0.986	8	12–13
0.004	775	1350	1.48	0.60	0.939	8	12–13
0.005	750	810	1.48	0.60	0.921	8	10–11
0.005	750	810	1.48	0.60	0.872	8	10–11
0.005	750	810	1.48	0.60	0.882	8	10–11
0.005	750	810	1.48	0.60	0.950	...	...
0.010	690	405	1.48	0.60	1.033	7	8–9
0.010	690	405	1.48	0.60	1.172	7	8–9
0.010	690	405	1.48	0.60	0.980	7	8–9
0.010	690	405	1.48	0.60	1.118	7	8–9
0.010	690	405	1.48	0.60	1.102	...	8–9
0.005	750	750	1.82	0.70	0.960	...	...
0.010	690	375	1.82	0.70	1.065	...	...

yield higher values of the axial buckling coefficient. Thus the interaction curves for cylinders undoubtedly depend on the radius-thickness ratio of the cylinder and would require many more tests for their detailed establishment. However, from the limited data, we may conclude that the use of a straight line interaction curve, or the theoretical curve, is conservative and, considering the wide range of values that might be expected for cylinders having a given radius-thickness ratio, is adequate for design.

The behavior of the few cones tested was quite different in that an unexpected phenomenon was encountered. Although the load carrying capacity of cylinders always decreased when buckling occurred (with the buckle mode remaining the same), such is not the case for conical shells. It was found that, for low values of external pressure, two distinct equilibrium shapes could be obtained for approximately the same axial compressive load. For larger values of the external pressure, the mode associated with buckling

Table 1 Continued

t, in.	$E \times 10^{-3}$, psi	ρ_{av}/t	l/ρ_{av}	$1 - R_1/R_2$[c]	p_{cr}/p_e	n (experimental)	n (predicted)
			c) $\alpha = 45°$				
0.005	750	1270	0.22	0.20	0.843	20	22–23
0.005	750	1270	0.22	0.20	0.784	21	22–23
0.003	775	1765	0.67	0.50	0.854	13	14–15
0.003	775	1765	0.67	0.50	0.910	12	14–15
0.002	740	1875	1.82	0.70	0.954	8	11–12
0.002	740	1875	1.82	0.70	0.954	8	11–12
0.003	775	1530	1.08	0.70	1.034	9	11–12
0.003	775	1530	1.08	0.70	1.015	9	11–12
0.005	750	918	1.08	0.70	1.002	...	...
0.005	750	918	1.08	0.70	0.978	...	...
0.010	690	459	1.08	0.70	1.142	...	...
0.010	690	459	1.08	0.70	1.215	...	...
0.010	690	459	1.08	0.70	1.134	...	...
0.002	740	2030	1.48	0.85	0.993	9	10–11
0.002	740	2030	1.48	0.85	1.053	10	10–11
0.003	775	1353	1.48	0.85	0.863	10	9–10
0.003	775	1353	1.48	0.85	0.910	10	9–10
0.005	750	812	1.48	0.85	1.029	8	8–9
0.005	750	812	1.48	0.85	0.951	8	8–9
0.005	750	812	1.48	0.85	0.932	...	8–9
0.005	750	812	1.48	0.85	0.928	...	8–9
0.005	750	812	1.48	0.85	0.960	...	8–9
0.010	690	406	1.48	0.85	1.044	6	7
0.010	690	406	1.48	0.85	1.065	6	7
0.010	690	406	1.48	0.85	1.181	...	7
0.010	690	406	1.48	0.85	1.181	...	7
0.010	690	406	1.48	0.85	1.251	...	7

[a] $R = 4$ in. in all cases.
[b] $R_2 = 5$ in. in all cases.
[c] $R_2 = 5$ in. in all cases.

Table 2 Experimental data for steel cylinders and cones under external uniform hydrostatic pressure

t, in.	$E \times 10^{-6}$, psi	ρ_{av}/t	l/ρ_{av}	$1 - R_1/R_2$[a]	p_{cr}/p_e	n (experimental)	n (predicted)
			$\alpha = 0°$				
0.010	30.3	800	1	0	0.928	12	14
0.010	30.3	800	2	0	0.930	8	10
0.010	30.3	800	2	0	1.015	8	10
0.010	30.3	800	1	0	0.970	12	14
			$\alpha = 30°$				
0.010	30.3	810	1.48	0.60	1.270	9	10–11
0.010	30.3	810	1.48	0.60	1.250	10	10–11
0.020	30.3	405	1.48	0.60	1.108	9	8–9
0.020	30.3	405	1.48	0.60	0.982	9	8–9
			$\alpha = 60°$				
0.010	30.3	1500	0.38	0.50	0.937	11	13–14
0.010	30.3	1500	0.38	0.50	0.904	11	13–14
0.010	30.3	1300	0.62	0.70	0.959	8	10
0.010	30.3	1300	0.62	0.70	1.105	9	10
0.010	30.3	1200	0.77	0.80	0.970	7	9
0.010	30.3	1200	0.77	0.80	1.200	8	9
0.020	30.3	600	0.77	0.80	1.045	6	7–8
			$\alpha = 75°$				
0.020	30.3	1255	0.29	0.70	0.989	...	7–8
0.010	30.3	2318	0.36	0.80	0.941	8	8–9
0.010	30.3	2318	0.36	0.80	0.973	9	8–9
0.010	30.3	2318	0.36	0.80	0.971	9	8–9
0.020	30.3	1159	0.36	0.80	1.130	8	6–7

[a] $R_2 = 8$ in. for cylinders and 10 in. for cones.

was first obtained as the axial load was increased. When buckling occurred, the load carrying capacity would drop slightly but then would continue to increase beyond the buckling load until the second mode, called the collapse mode, was obtained. In addition, the cones continued to carry some load when the pressure was increased beyond the critical value for external pressure alone, decreasing finally to zero when the external pressure that would yield the collapse mode was reached.

An illustration of the buckle and collapse modes of conical shells for various external pressures is shown in Fig. 6. It is interesting to note that, except for the case of axial compression alone, the buckle mode shape does not vary much with external pressure and that the collapse mode can be considered to be independent of load. The buckling behavior differs somewhat from that associated with cylinders, for which the buckled shapes are illustrated in Fig. 7.

The experimental data for the conical shells are shown in Figs. 8 and 9. In addition to a parameter involving the buckling load P, another parameter for the collapse load P^1 is given. The curves for P/P_0 and P^1/P_0 as a function of p/p_0 are shown in Fig. 8 for the 30° cones and in Fig. 9 for the 60° cones. It can be seen that the different physical behavior of conical shells is associated with interaction curves that differ from those for cylinders. The buckling data for the various cones are in fairly good agreement with the theoretically predicted interaction curves. The collapse data indicate that the phenomenon is a function of the semivertex angle since the collapse loads for the 30° cones differ from the buckling loads at pressures greater than about 60% of the critical value for pressure alone, compared to pressures greater than about 20% of the critical value for pressure alone for the 60° cones. The 60° cones are also seen to have collapse load ratios larger than those for 30° cones, as well as a larger collapse pressure ratio.

When the values of $P/2\pi Et^2 \cos^2\alpha$ are plotted as a function of p/p_0 (Fig. 10), it can be seen that, even though the axial load coefficient for axial load alone is of the same order as

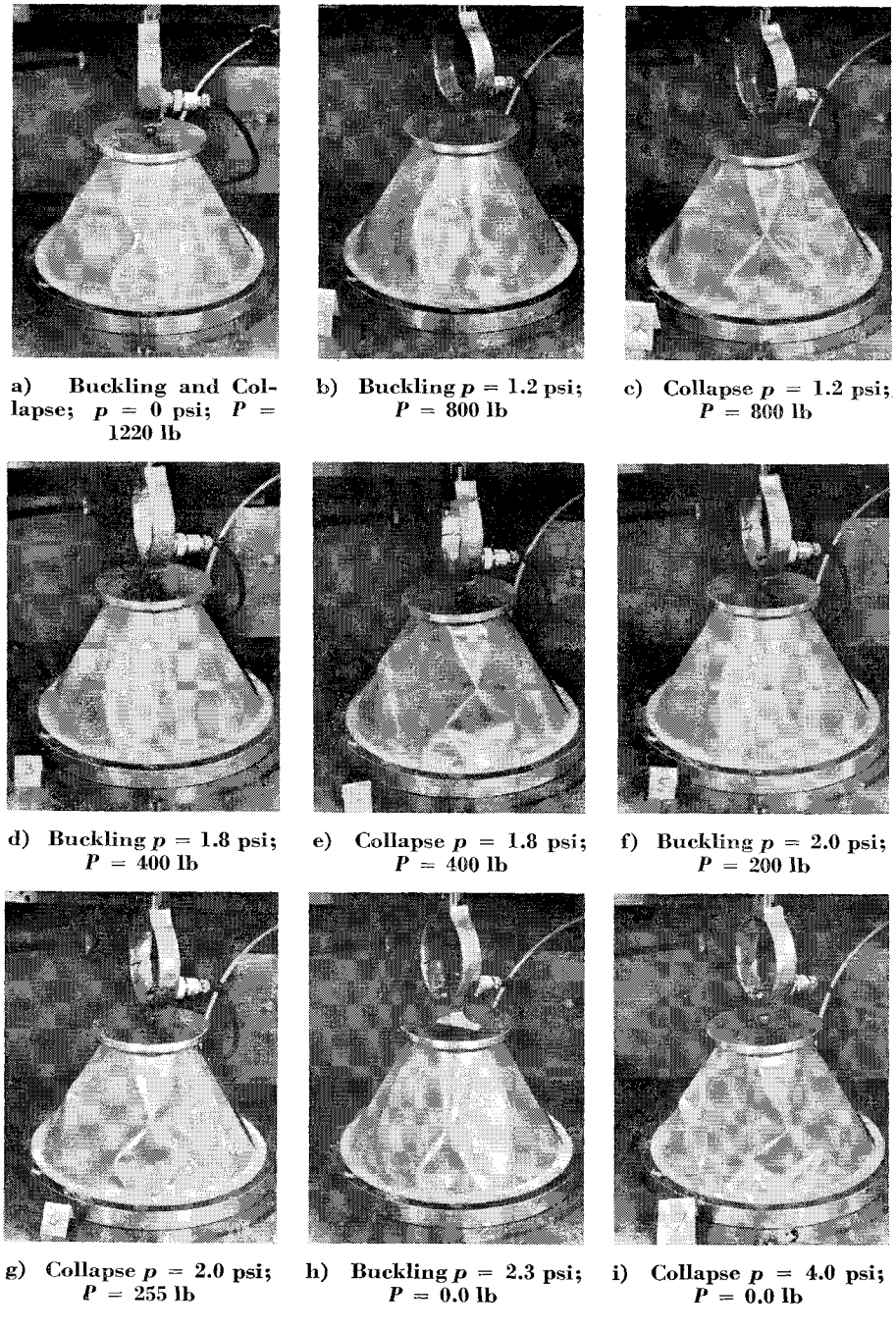

a) Buckling and Collapse; $p = 0$ psi; $P = 1220$ lb

b) Buckling $p = 1.2$ psi; $P = 800$ lb

c) Collapse $p = 1.2$ psi; $P = 800$ lb

d) Buckling $p = 1.8$ psi; $P = 400$ lb

e) Collapse $p = 1.8$ psi; $P = 400$ lb

f) Buckling $p = 2.0$ psi; $P = 200$ lb

g) Collapse $p = 2.0$ psi; $P = 255$ lb

h) Buckling $p = 2.3$ psi; $P = 0.0$ lb

i) Collapse $p = 4.0$ psi; $P = 0.0$ lb

Fig. 6 Variation of buckle and collapse patterns for a conical shell with different combinations of axial compression and external pressure.

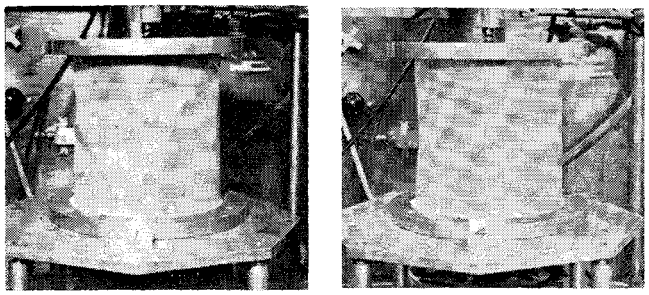

a) $P/P_0 = 1$, $p/p_0 = 0$ d) $P/P_0 = 0.46$, $p/p_0 = 0.6$

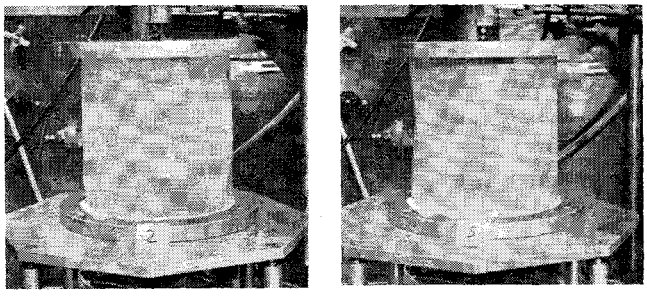

b) $P/P_0 = 0.74$, $p/p_0 = 0.2$ e) $P/P_0 = 0.30$, $p/p_0 = 0.7$

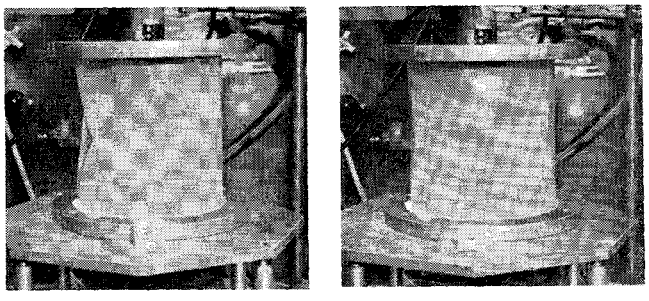

c) $P/P_0 = 0.54$, $p/p_0 = 0.4$ f) $P/P_0 = 0$, $p/p_0 = 1$

Fig. 7 Variation of buckle pattern for cylinders with different combinations of axial compression and external pressure.

those for the smaller radius-thickness ratio cylinders, the shapes of the curves are quite different. The cone data indicate a percentage reduction in the axial load parameter which is almost independent of the pressure ratio (hence, yielding almost a straight line interaction curve), whereas the cylinder data (Fig. 5) indicate agreement between theory and experiment for pressure ratios near unity and an insensitivity to pressure for pressure ratios near zero.

It is evident that considerable theoretical and experimental work remains to be done to explain the differences between cone and cylinder behavior under combined axial compression

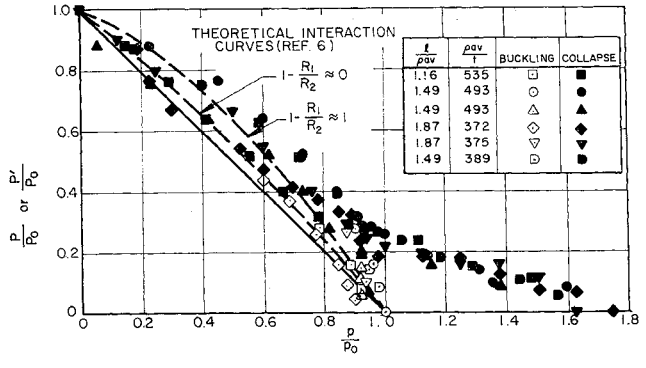

Fig. 8 Interaction curves for 30° cones under axial compression and external uniform hydrostatic pressure.

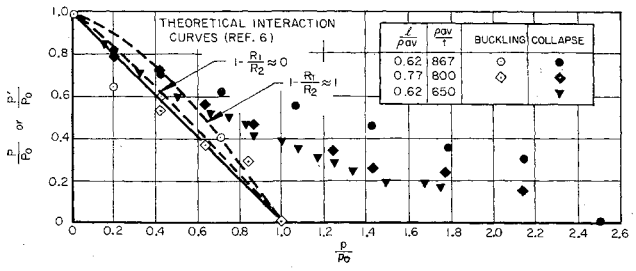

Fig. 9 Interaction curves for 60° cones under axial compression and external uniform hydrostatic pressure.

and external pressure. The limited results do indicate, however, that a straight line interaction curve is safe for design purpose.

Concluding Remarks

For external pressure alone, the experimental results indicate that for conservative design the critical pressure for cylinders and cones should be taken as

$$p_{cr} = \frac{0.74E}{(l/\rho_{av})(\rho_{av}/t)^{5/2}} \quad (4$$

which is about 80% of the theoretical value for cylinders and 66–80% of the theoretical value for cones. An average value for the test data is obtained by increasing the factor of 0.74 in Eq. (4) to a value of 0.92. Future study in areas of interest indicated by these results call for a complete explanation of the rather wide scatter band and the discrepancy between theory and experiment that is larger for conical shells than for cylinders.

Interaction curves between external pressure and axial compression indicate that for cylinders the results depend on the radius-thickness ratio and possibly the length-radius ratio. A straight line interaction curve is conservative. For conical shells we have the unexplained phenomenon of a differentiation between buckling and collapse loads. The buckling interaction curves appear to follow an almost straight line, indicating an unexpected uniform percentage decrease in the axial compressive load from the theoretical value, whereas the collapse interaction curve appears to depend on the semi-vertex angle of the cone. Additional tests and theoretical investigations are needed for a definitive description of the phenomena.

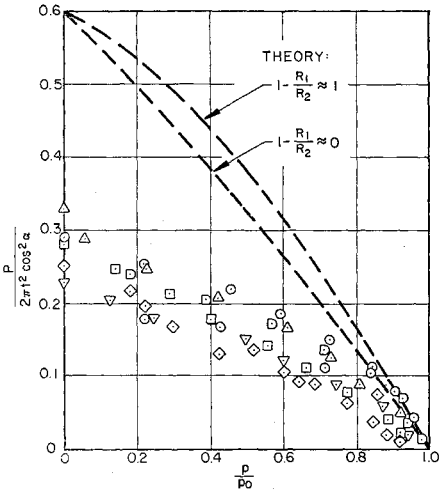

Fig. 10 Variation of axial compression coefficient with external pressure ratios for 30° and 60° cones.

References

[1] Seide, P., "On the buckling of truncated conical shells under uniform hydrostatic pressure," *Proceedings of the I.U.T.A.M. Symposium on the Theory of Thin Elastic Shells, Delft, 24–25 August, 1959* (North-Holland Publishing Co., Amsterdam, 1960), pp. 363–388.

[2] Niordson, F. I. N., "Buckling of conical shells subjected to uniform external lateral pressure," Trans. Roy. Inst. Technol., Stockholm **10,** 1–12 (1947).

[3] Bijlaard, P. P., "Critical external pressure of conical shells that are simply supported at the edges," Bell Aircraft Corp., TR 02-941-027 (February 1953).

[4] Timoshenko, S., *Theory of Elastic Stability* (McGraw-Hill Book Co., Inc., New York, 1936), pp. 439–443.

[5] Flügge, W., "Die Stabilitat der Kreiszylinderschale," Ingr.-Arch. **3,** 436–506 (1932).

[6] Seide, P., "The stability of thin conical frustums subjected to axial compression and external pressure," TRW Space Technology Labs., Inc. (1960); unpublished.

[7] Seide, P., Weingarten, V. I., and Morgan, E. J., "Final report on the development of design criteria for elastic stability of thin shell structures," Space Technology Laboratories, Rept. STL/TR-60-0000-19425 (December 1960).

[8] Batdorf, S. B., "A simplified method of elastic-stability analysis for thin cylindrical shells, I-Donnell's equation," NACA TN 1341 (June 1947).

[9] Windenberg, D. F. and Trilling, C., "Collapse by instability of thin cylindrical shells under external pressure," Trans. Am. Soc. Mech. Engrs. **56,** 819–825 (1934).

[10] Sturm, R. G., "A study of the collapsing pressure of thin-walled cylinders," Engineering Experiment Station, Univ. of Illinois, Bull. 329 (1941).

[11] Tokugana, T., "Experiments on the elastic stability of a thin-wall cone under uniform normal pressure on all sides, and an approximate method for computing its collapsing pressure," Applied Mechanics League, Congress Shipbuilding Association, Japan Miscellaneous Publ. 125, pp. 151–169 (1932).

[12] Harris, W. F. and Leyland, J., "The strength of conical vessels subject to external pressure," Trans. Inst. Chem. Engrs. (London) **30,** 65–74 (1952).

[13] Magula, A. W., "Structural test-conical head assembly, test no. 815," North American Aviation, Inc., Missile Test Lab. Rept. MTL-531 (1954).

[14] Westmoreland, R. T., "Model test of conical bulkhead, test no. 1098," North American Aviation, Inc., Missile Test Lab. Rept. MTL-652 (1955).

[15] Jordan, W. D., "Buckling of thin conical shells under uniform external pressure," Bureau of Engineering Research, College of Engineering, Univ. of Alabama, Technical Report (February 1955).

[16] Bowie, O. L., Parker, B. S., Radkowski, P. P., and Bluhm, J. I., "A study of the IRBM (Jupiter) bulkheads," Watertown Arsenal Labs. Rept. 880–54 (August 1956).

[17] Shroeder, F. J., Kusterer, E. T., and Hirsch, R. A., "An experimental determination of the stability of conical shells," Aircraft Armaments, Inc., Rept. ER-1361 (May 1958).

[18] Homewood, R. H., Brine, A. C., and Johnson, A. E., "Buckling instability of monocoque shells," Avco TR Rad-TR-9-59-20 (August 1959).

[19] Kempner, J., 10th International Congress of Theoretical and Applied Mechanics (1960); unpublished.